

---Supporting Information---

**Electrocatalytic amino acid synthesis from biomass-  
derivable keto acids over ball milled carbon nanotubes**

Yiying Xiao<sup>†,‡</sup>, Chia Wei Lim<sup>‡</sup>, Jinqun Chang<sup>†,‡</sup>, Qixin Yuan<sup>‡</sup>, Lei Wang<sup>\*‡</sup>, Ning Yan<sup>\*†,‡</sup>

<sup>†</sup>*Joint School of National University of Singapore and Tianjin University, International  
Campus of Tianjin University, Binhai New City, Fuzhou 350207, China*

<sup>‡</sup>*Department of Chemical and Biomolecular Engineering, National University of  
Singapore, Singapore 117585, Singapore*

\*Corresponding authors:

Lei Wang, Department of Chemical and Biomolecular Engineering, National University  
of Singapore, Singapore, 117585. Email: [wanglei8@nus.edu.sg](mailto:wanglei8@nus.edu.sg)

Ning Yan, Department of Chemical and Biomolecular Engineering, National University  
of Singapore, Singapore, 117585. Email: [ning.yan@nus.edu.sg](mailto:ning.yan@nus.edu.sg)

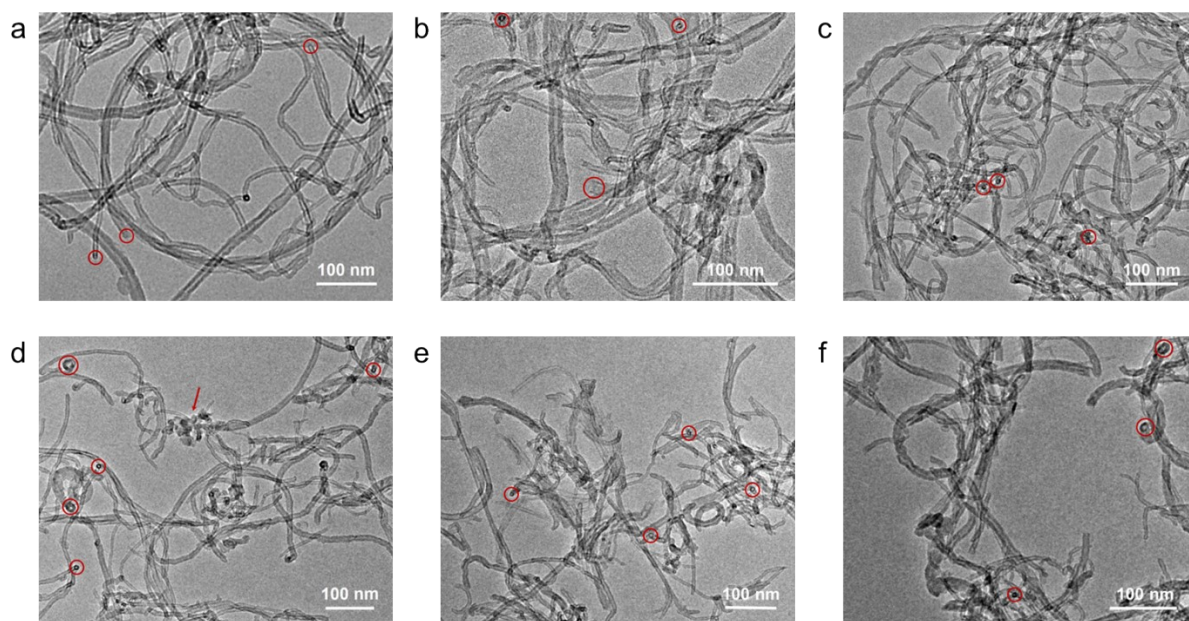
**Table of Contents**

Number of pages in the supporting information: 29

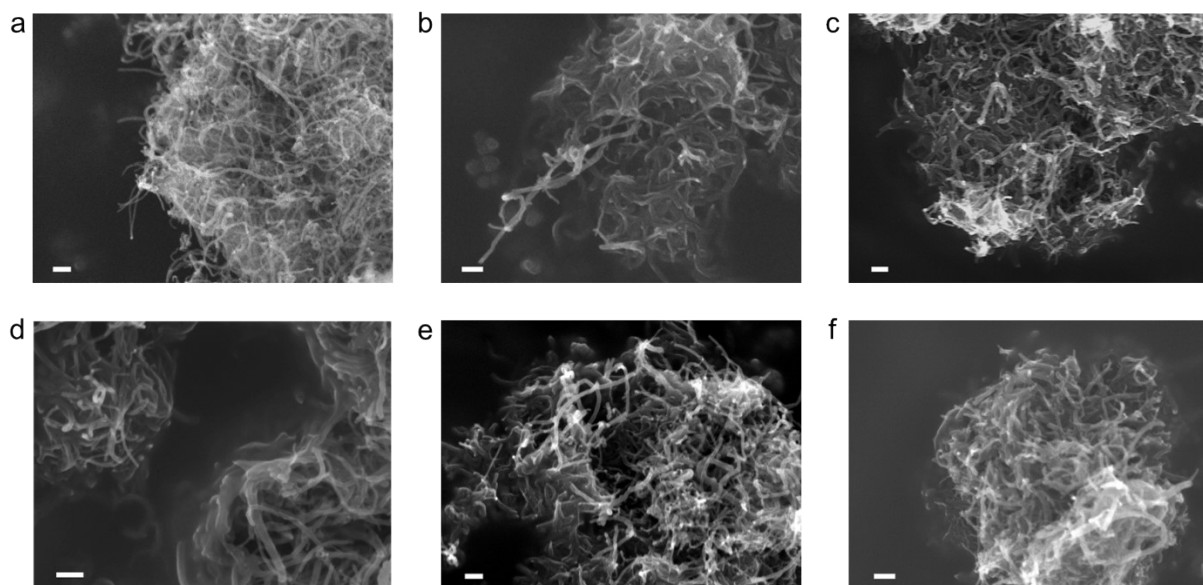
Number of figures in the supporting information: 18

Number of tables in the supporting information: 3

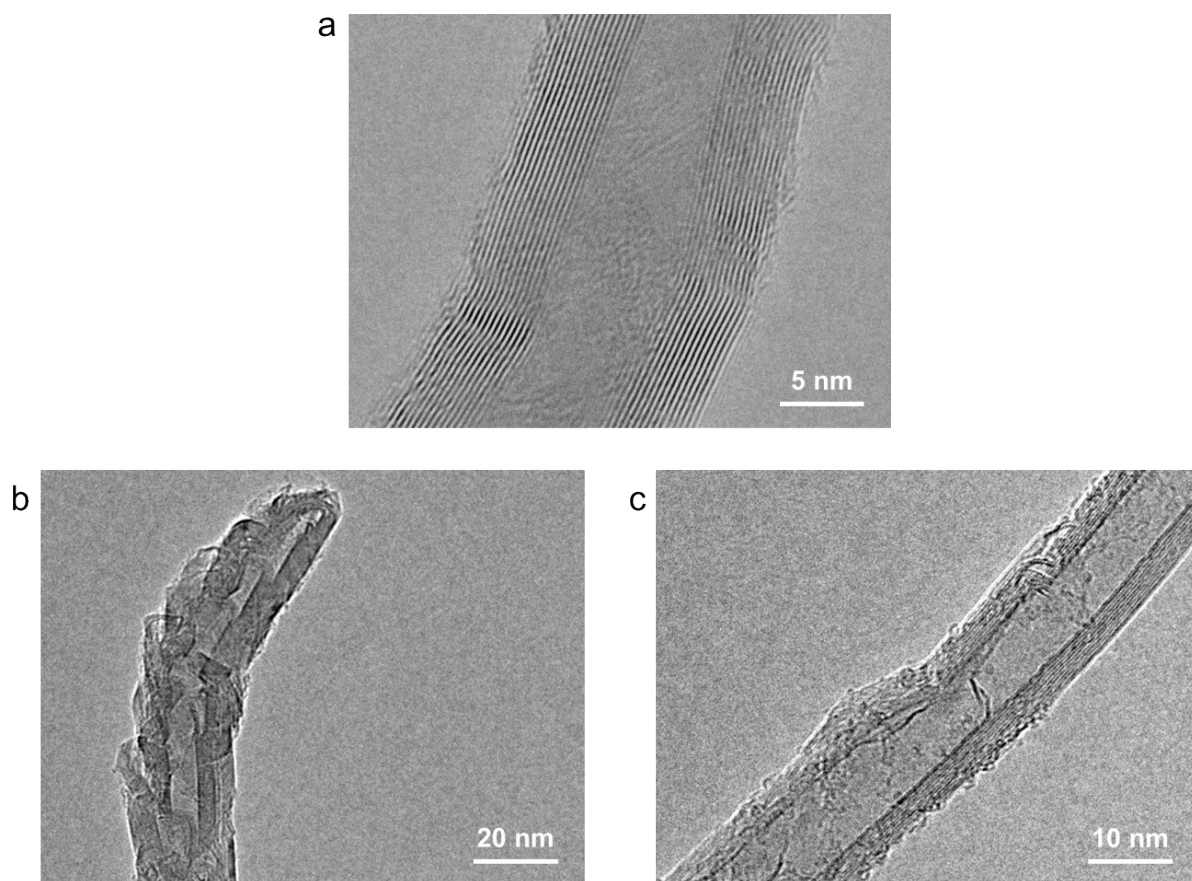
Number of schemes in the supporting information: 2



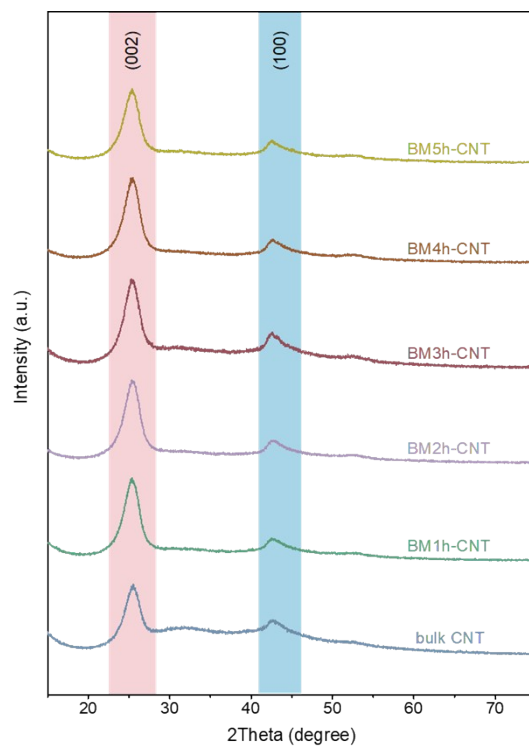
**Figure S1** TEM images of **a)** bulk CNT, **b)** BM1h-CNT, **c)** BM2h-CNT, **d)** BM3h-CNT, **e)** BM4h-CNT and **f)** BM5h-CNT.



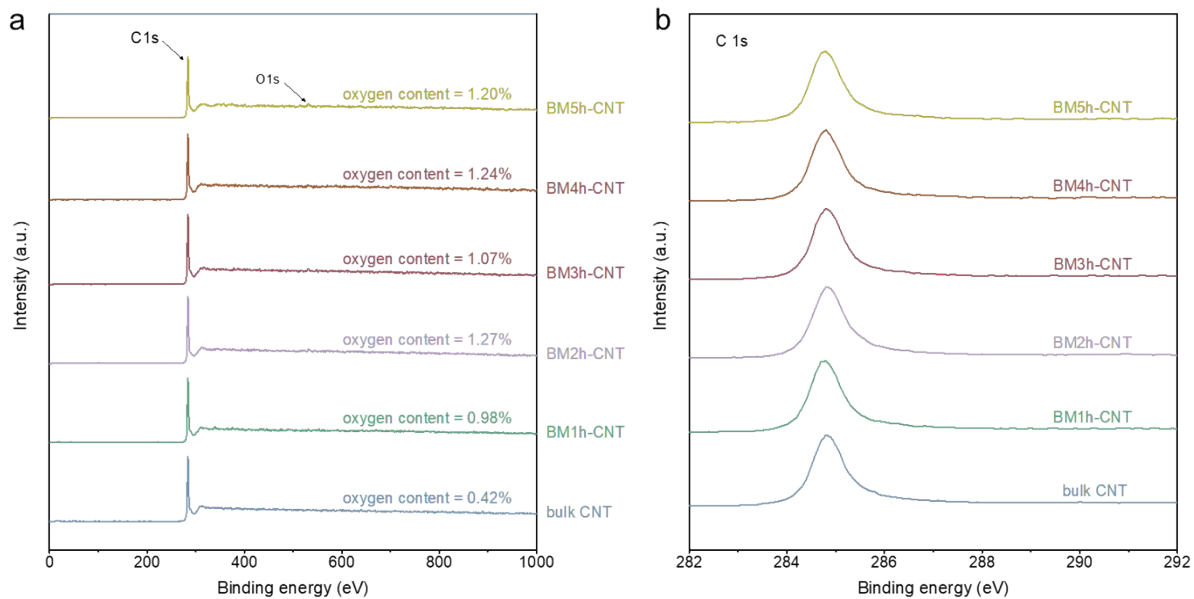
**Figure S2** SEM images of **a)** bulk CNT, **b)** BM1h-CNT, **c)** BM2h-CNT, **d)** BM3h-CNT, **e)** BM4h-CNT and **f)** BM5h-CNT (scale bar: 100 nm).



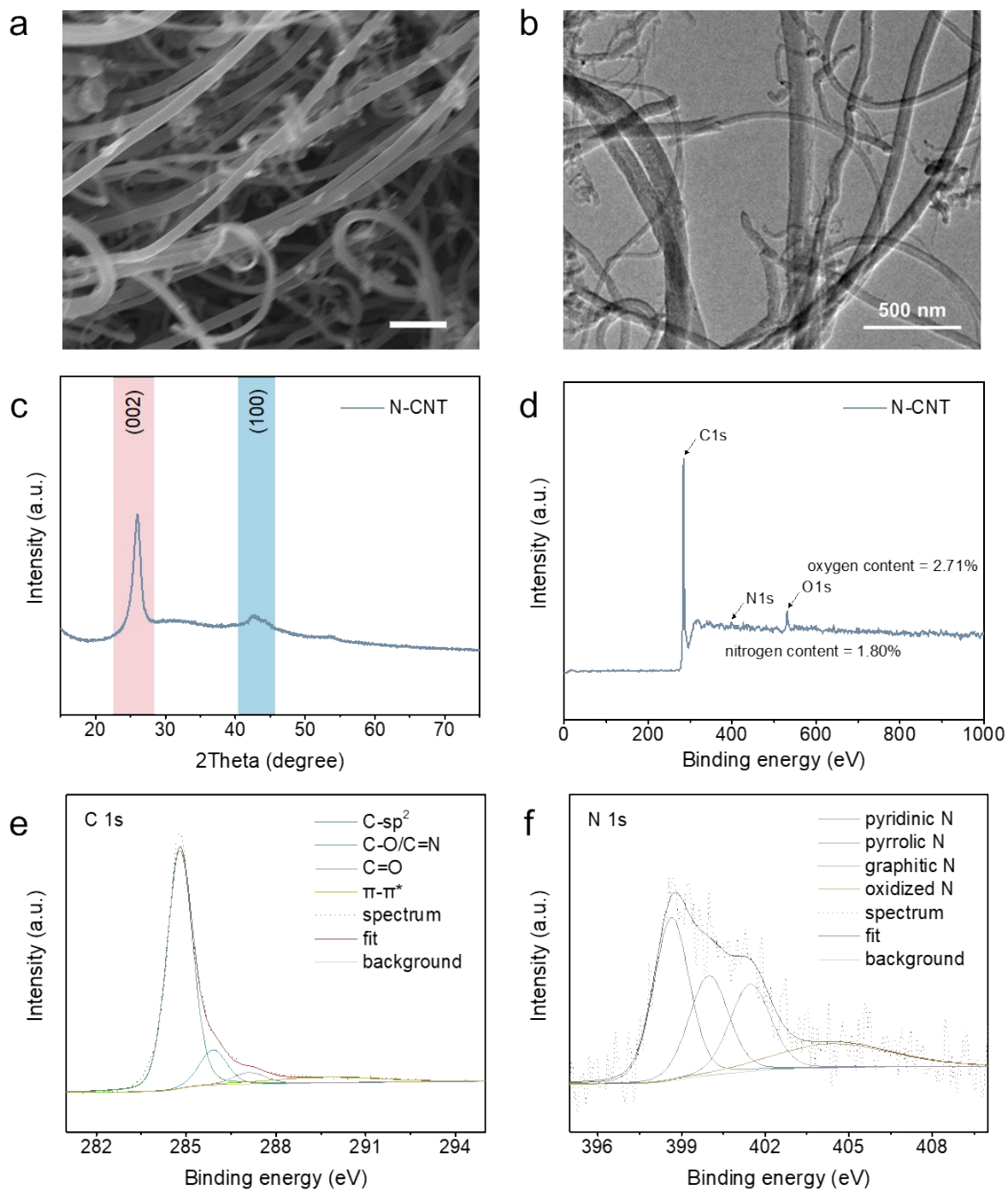
**Figure S3** High resolution transmission electron microscopy (HRTEM) images of **a)** bulk CNT and **b, c)** BM3h-CNT.



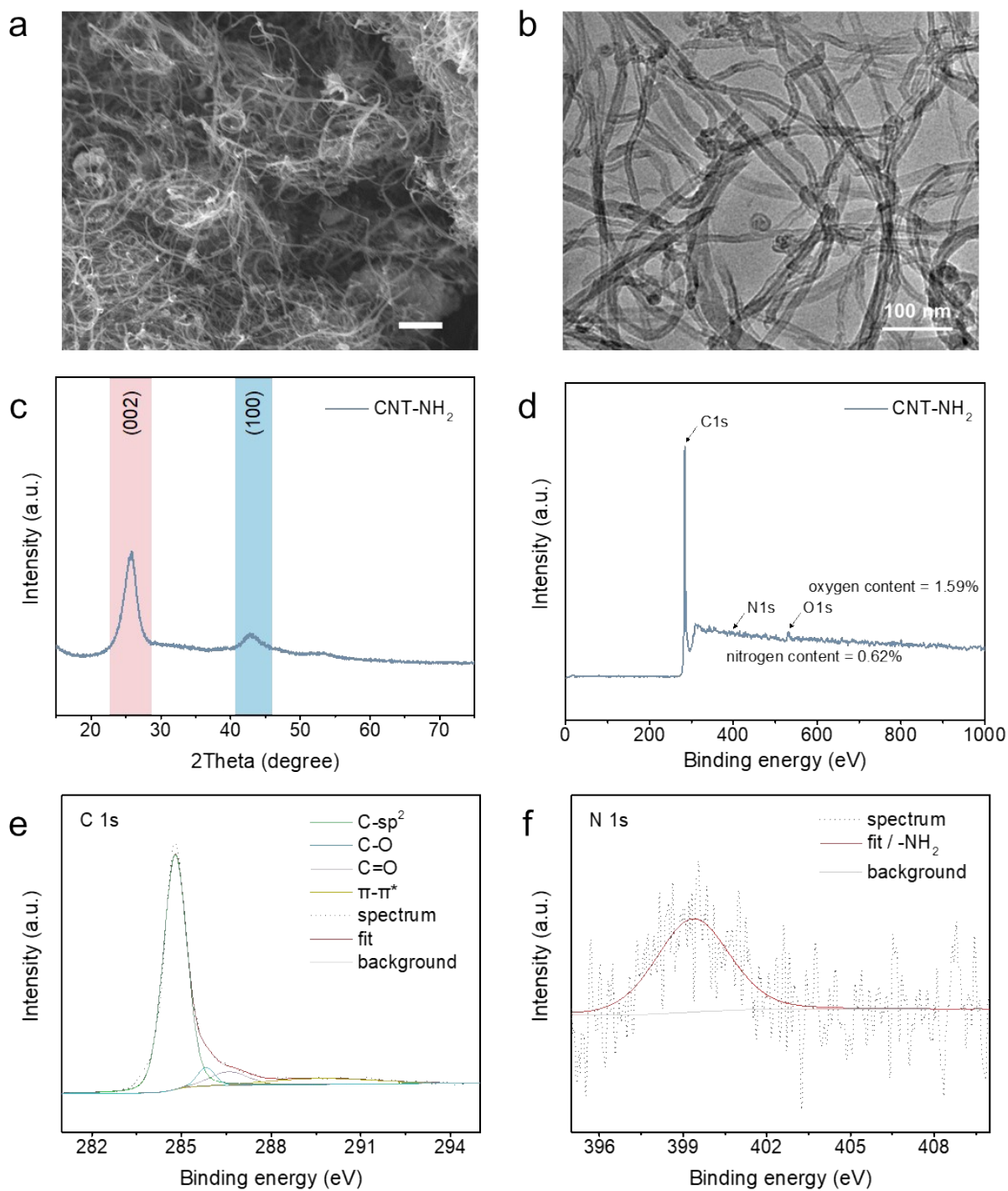
**Figure S4** XRD patterns of bulk CNT and BMXh-CNTs (X = 1, 2, 3, 4, 5).



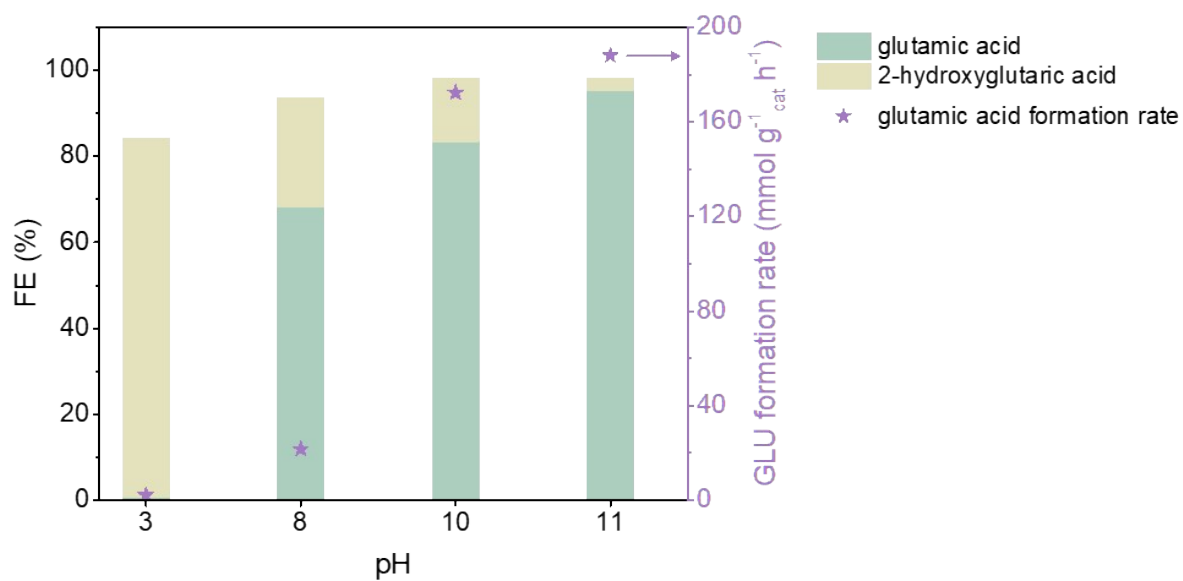
**Figure S5 a)** XPS survey spectra and **b)** XPS high resolution C 1s spectra of bulk CNT and BMXh-CNTs (X = 1, 2, 3, 4, 5).



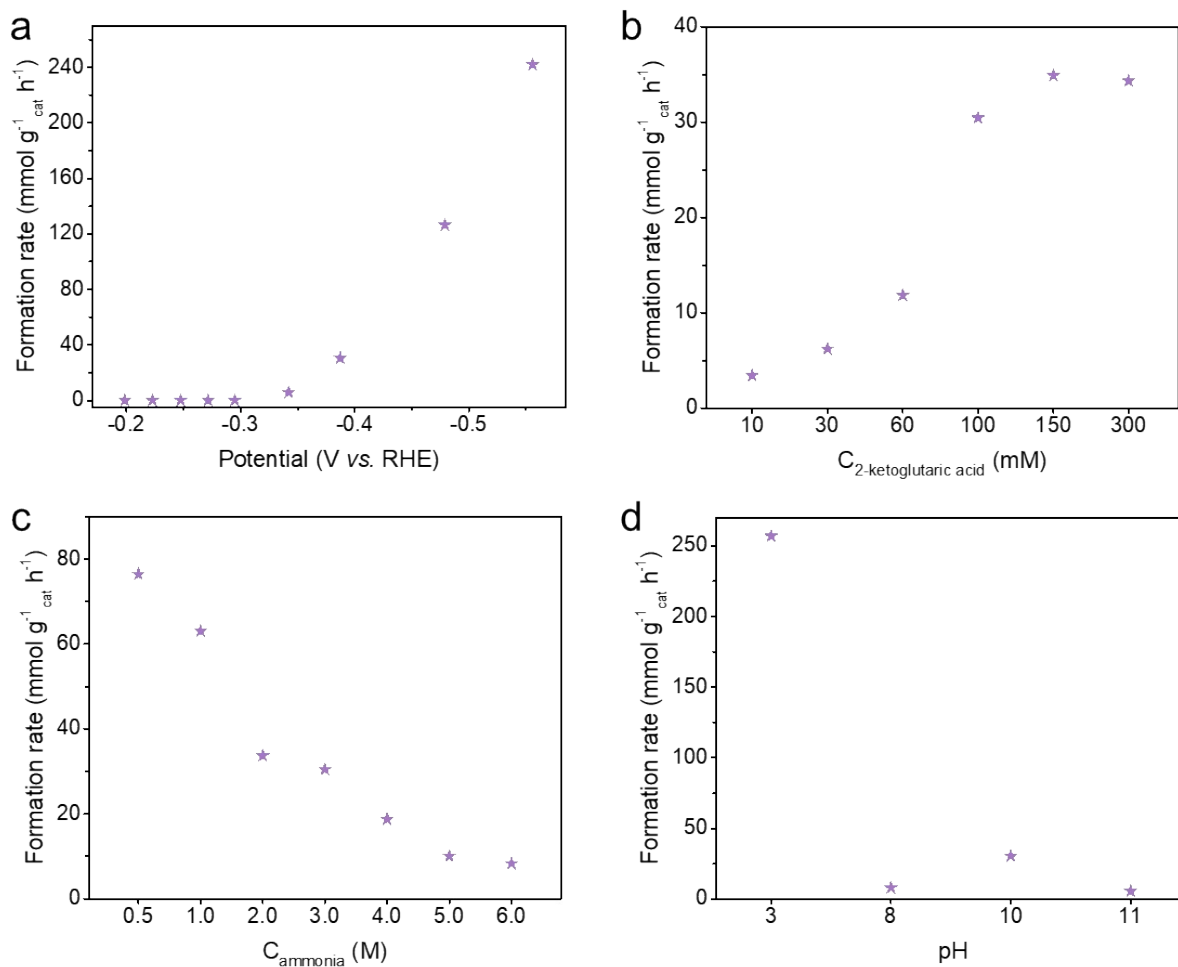
**Figure S6 Physical characterizations of N-CNT. a)** SEM image (scale bar: 500 nm). **b)** TEM image. **c)** XRD pattern. The peaks at around 25.4° and 42.6° are attributed to the (002) graphite plane reflection and (100) in plane reflection, respectively. **d)** XPS survey spectra. **e)** XPS high resolution C 1s spectra. **f)** XPS high resolution N 1s spectra.



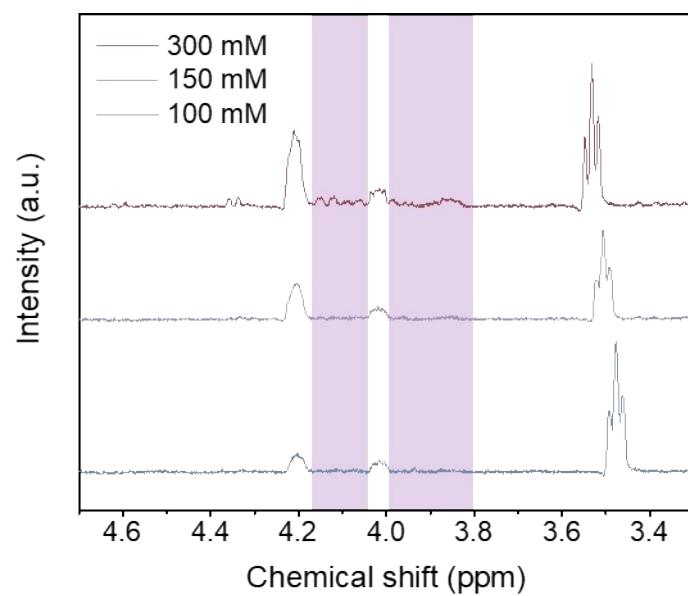
**Figure S7 Physical characterizations of CNT-NH<sub>2</sub>.** **a)** SEM image (scale bar: 500 nm). **b)** TEM image. **c)** XRD pattern. The peaks at around 25.4° and 42.6° are attributed to the (002) graphite plane reflection and (100) in plane reflection, respectively. **d)** XPS survey spectra. **e)** XPS high resolution C 1s spectra. **f)** XPS high resolution N 1s spectra.



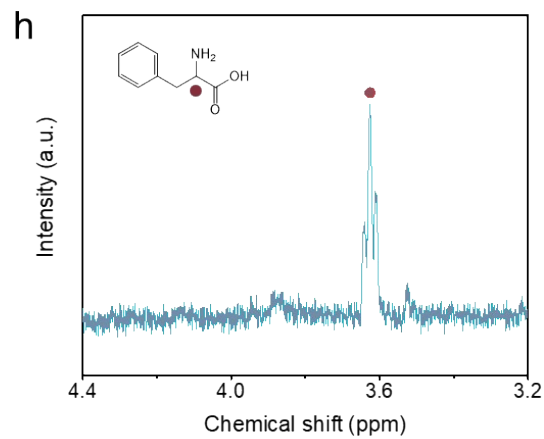
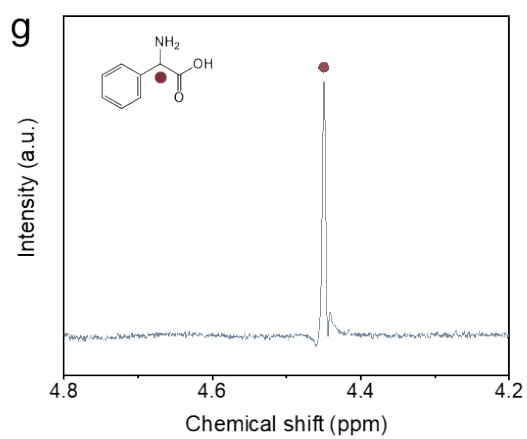
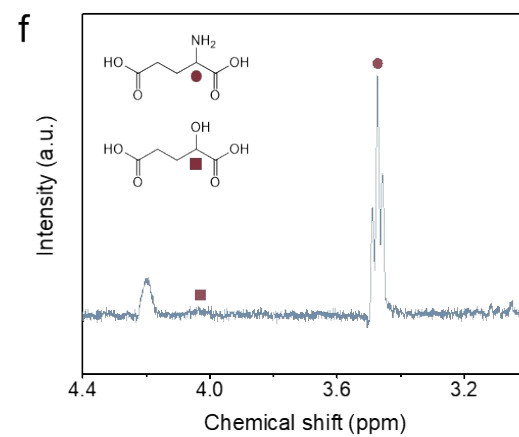
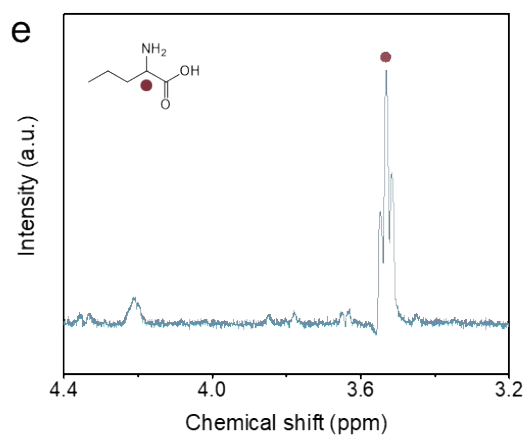
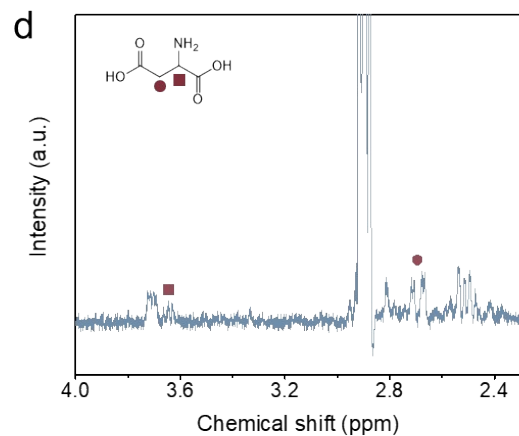
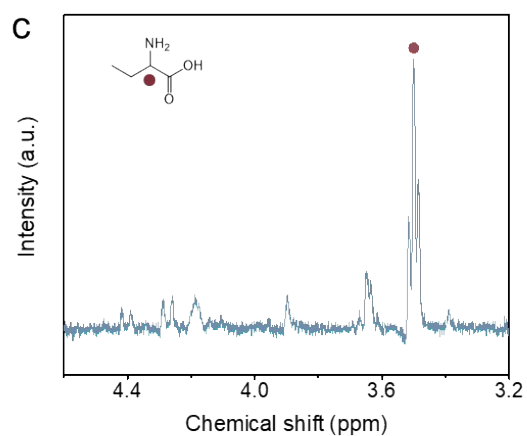
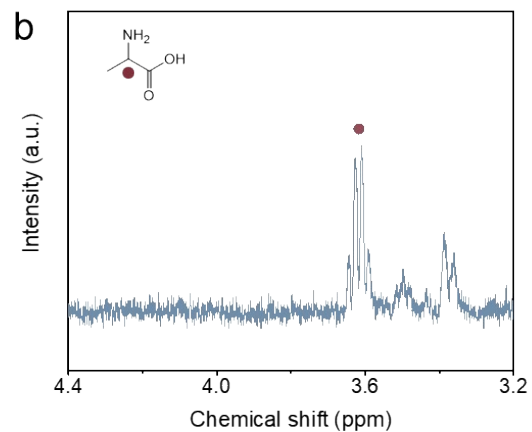
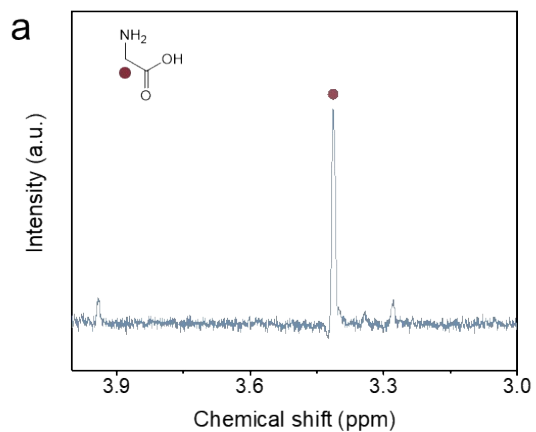
**Figure S8** Faradaic efficiencies and glutamic acid formation rate of the BM3h-CNT catalysed room-temperature constant potential electrolysis of 2-ketoglutaric acid under different pH ( $-0.39$  V vs. RHE, 100 mM 2-ketoglutaric acid, 6 M  $\text{NH}_3/\text{NH}_4^+$ , 1 h reaction time).



**Figure S9** Formation rate of 2-hydroxyglutaric acid during the BM3h-CNT catalysed room-temperature constant potential electrolysis of 2-ketoglutaric acid for 1 h under different **a)** applied potentials (100 mM 2-ketoglutaric acid, 3 M NH<sub>3</sub>, pH 10), **b)** 2-ketoglutaric acid concentrations (-0.39 V vs. RHE, 3 M NH<sub>3</sub>, pH 10), **c)** NH<sub>3</sub> concentrations (-0.39 V vs. RHE, 100 mM 2-ketoglutaric acid, pH 10) and **d)** pH (-0.39 V vs. RHE, 100 mM 2-ketoglutaric acid, 6 M NH<sub>3</sub>/NH<sub>4</sub><sup>+</sup>).



**Figure S10** <sup>1</sup>H NMR spectra of reaction solutions for the synthesis of glutamic acid varying the substrate concentrations.



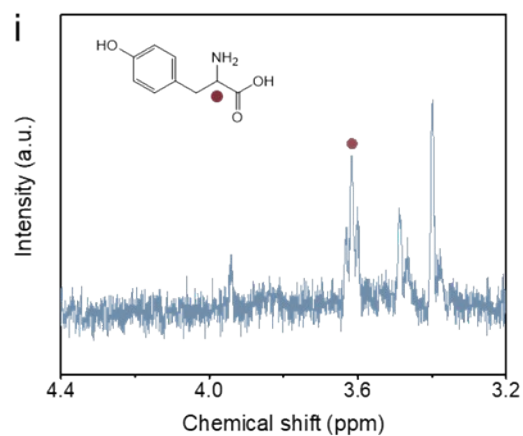


**Figure S11** <sup>1</sup>H NMR spectra of the reaction solutions for the synthesis of **a**) glycine, **b**) pyruvic acid, **c**) 2-aminobutyric acid, **d**) aspartic acid, **e**) norvaline, **f**) glutamic acid, **g**) phenylglycine, **h**) phenylalanine and **i**) tyrosine.

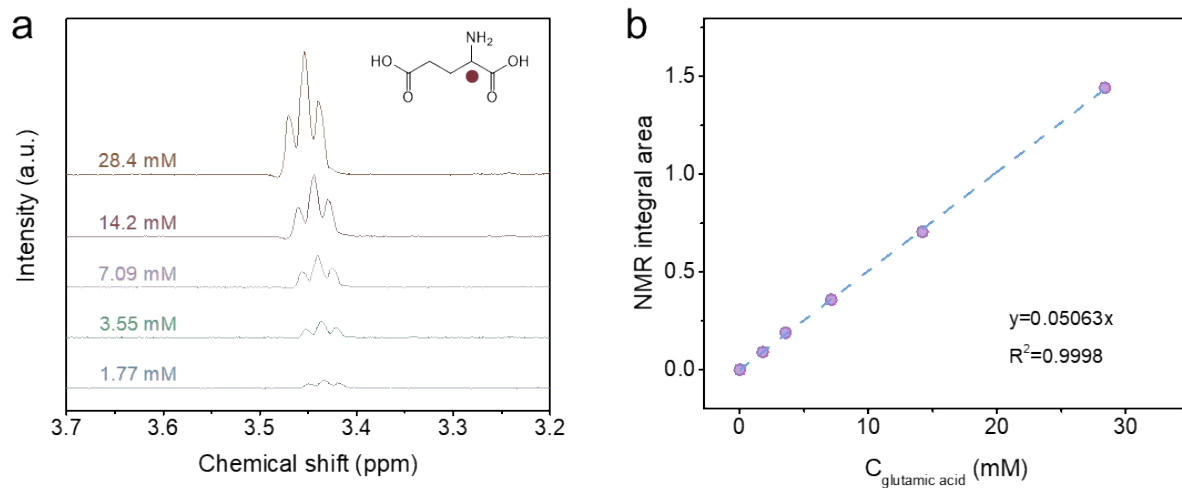


**Figure S12**  $^1\text{H}$  NMR spectra and calibration curve for quantification of glutamic acid. **a)**  $^1\text{H}$  NMR spectra of glutamic acid with various concentrations. **b)** The calibration curve for glutamic acid.

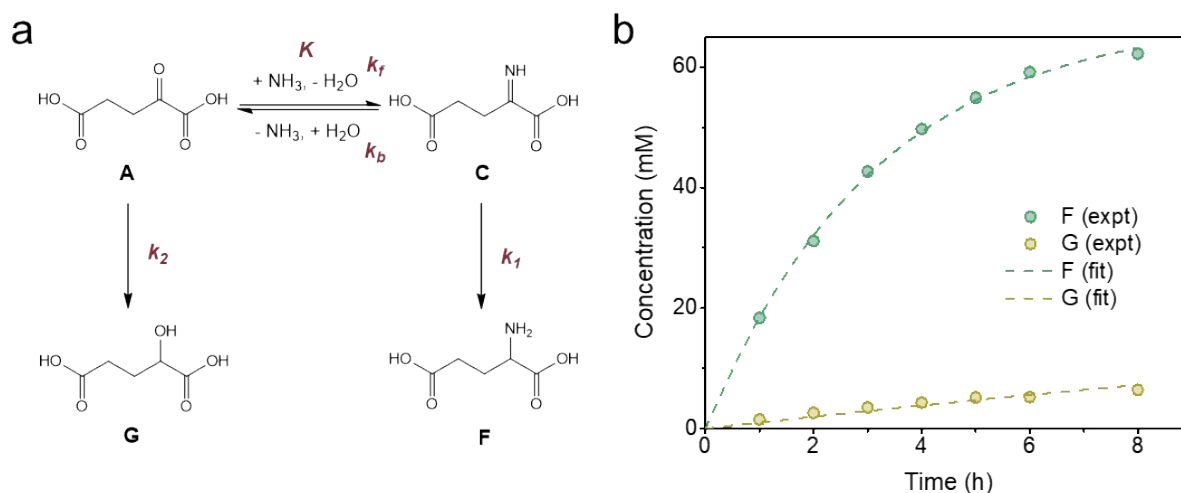


**Figure S13 Kinetic modelling of electrocatalytic reductive amination of 2-ketoglutaric acid. a)** Reaction pathway for the electro-reductive amination reaction used for modelling. **b)** Experimental results (circles) and kinetic model prediction (dashed lines) for the concentration profiles of glutamic acid (F) and 2-hydroxyglutaric acid (G) during extended duration electrolysis.

We have conducted kinetic modeling of the reaction to quantitatively verify the reaction pathway network and the rate-determining step we proposed. Based on our experimental results (Figure 5), the formation of glutamic acid is first order with respect to both 2-ketoglutaric acid and ammonia at low and moderate concentrations, and the rate determining step is the first electron transfer process. Thus, a simple reaction pathway as depicted in Figure S13a is used as the basis of the kinetic model.

Assume the ketone-imine chemical equilibrium is attained instantaneously at all time:

$$k_f[\text{NH}_3][\text{A}] \approx k_b[\text{C}] \Rightarrow K = \frac{[\text{C}]}{[\text{NH}_3][\text{A}]} = \frac{k_f}{k_b}$$

Rate equations for each species:

$$\frac{d[\text{A}]}{dt} = -k_2[\text{A}] - k_f[\text{NH}_3][\text{A}] + k_b[\text{C}] \approx -k_2[\text{A}] \Rightarrow [\text{A}] = [\text{A}]_{t=0} e^{-k_2 t}$$

$$\frac{d[\text{C}]}{dt} = k_f[\text{NH}_3][\text{A}] - k_b[\text{C}] - k_1[\text{C}] \approx -k_1[\text{C}] \Rightarrow [\text{C}] = [\text{C}]_{t=0} e^{-k_1 t}$$

$$\frac{d[\text{F}]}{dt} = k_1[\text{C}] = k_1[\text{C}]_{t=0} e^{-k_1 t} \Rightarrow [\text{F}] = [\text{C}]_{t=0} (1 - e^{-k_1 t})$$

$$\frac{d[\text{G}]}{dt} = k_2[\text{A}] = k_2[\text{A}]_{t=0} e^{-k_2 t} \Rightarrow [\text{G}] = [\text{A}]_{t=0} (1 - e^{-k_2 t})$$

The ketone-imine chemical equilibrium is attained instantaneously at  $t = 0$  with the added amount of A (concentration  $[\text{A}]_{\text{feed}}$ ):

$$K = \frac{[C]_{t=0}}{[NH_3][A]_{t=0}} \Rightarrow [C]_{t=0} = K[NH_3][A]_{t=0}$$

Mass balance for species A at  $t = 0$ :

$$[A]_{t=0} + [C]_{t=0} = [A]_{feed} \Rightarrow [C]_{t=0} = [A]_{feed} - [A]_{t=0}$$

Therefore:

$$K[NH_3][A]_{t=0} = [A]_{feed} - [A]_{t=0}$$

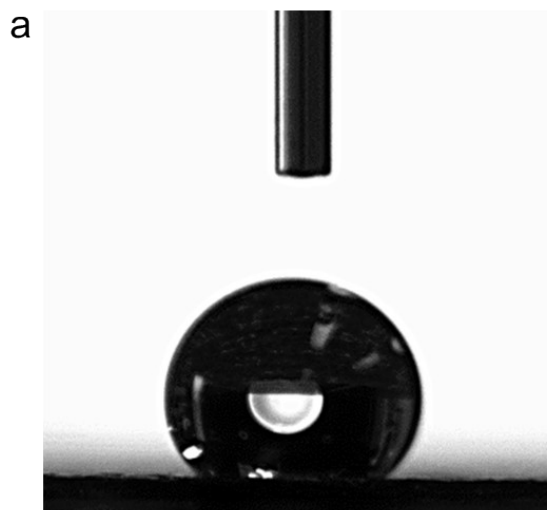
$$[A]_{t=0} = \frac{[A]_{feed}}{1 + K[NH_3]} \quad \text{and} \quad [C]_{t=0} = \frac{K[NH_3][A]_{feed}}{1 + K[NH_3]}$$

Concentration profiles for species F and G become:

$$[F] = \frac{K[NH_3][A]_{feed}}{1 + K[NH_3]} (1 - e^{-k_1 t})$$

$$[G] = \frac{[A]_{feed}}{1 + K[NH_3]} (1 - e^{-k_2 t})$$

Utilising our results for the extended duration electrolysis (Figure 3f), we use the method of least squares to obtain the fitted parameter values:  $K = 3.63 \times 10^{-4} \text{ mM}^{-1}$ ,  $k_1 = 0.318 \text{ h}^{-1}$ ,  $k_2 = 0.033 \text{ h}^{-1}$ . As shown in Figure S13b, the kinetic model prediction agrees reasonably well with the experimental results, implying that the model assumptions are justified under these reaction conditions.

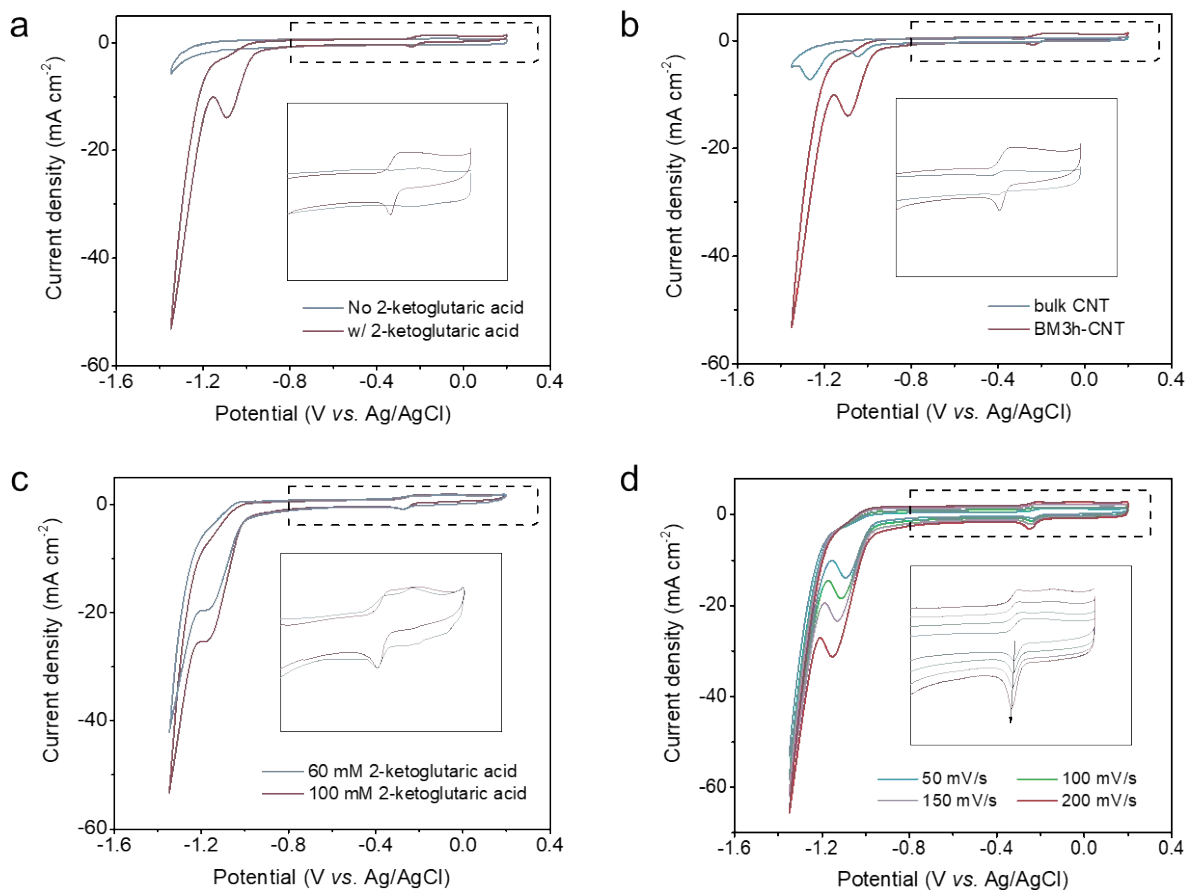


CA:  $125.1^\circ \pm 0.8^\circ$

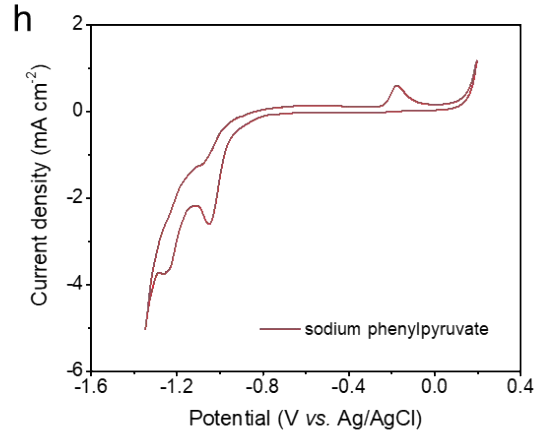
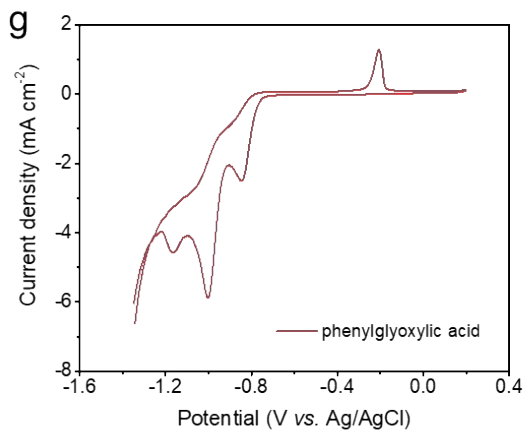
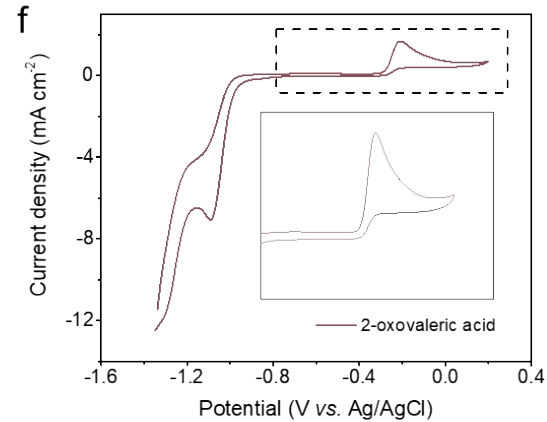
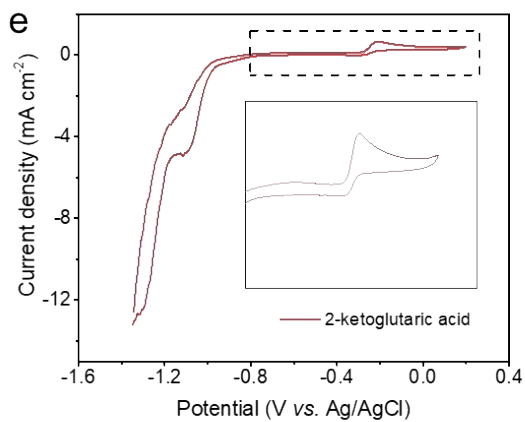
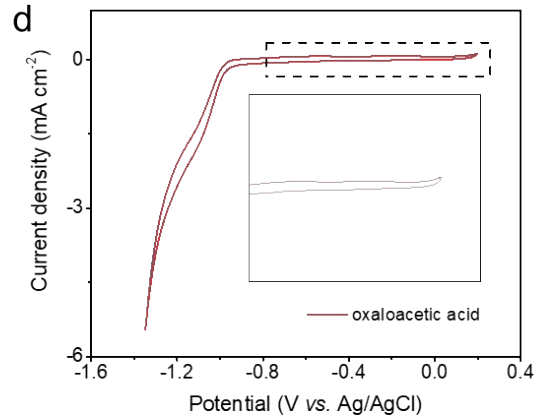
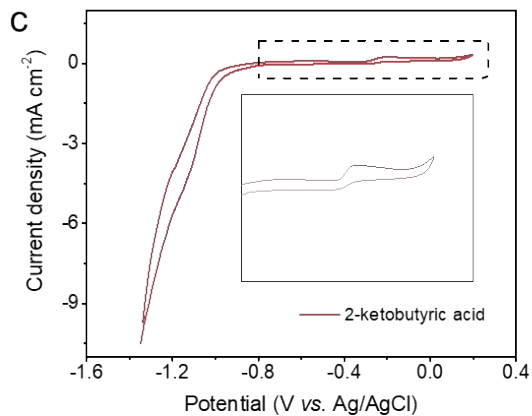
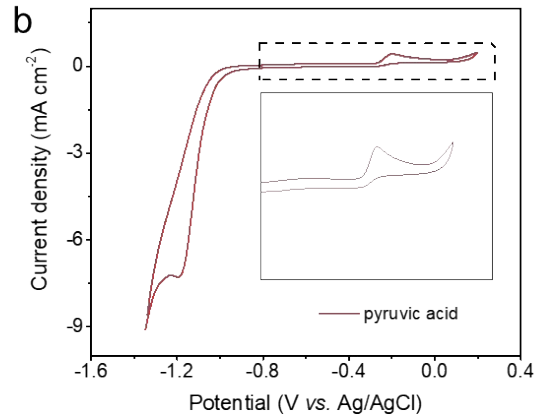
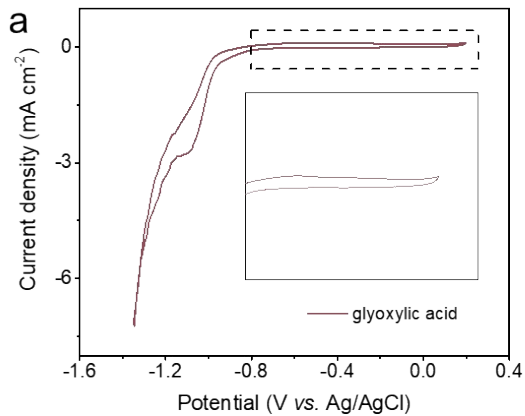


CA:  $132.2^\circ \pm 0.9^\circ$

**Figure S14** Contact angles (CAs) of **a**) carbon paper and **b**) carbon paper covered with BM3h-CNT. The values of CAs were averages calculated based on three independent measurements.



**Figure S15** CV curves of **a)** BM3h-CNT with and without 100 mM 2-ketoglutaric acid in a 3 M  $\text{NH}_3/\text{NH}_4^+$  buffer (pH 10) with a scan rate of 50 mV/s. **b)** bulk CNT or BM3h-CNT with 100 mM 2-ketoglutaric acid in a 3 M  $\text{NH}_3/\text{NH}_4^+$  buffer (pH 10) with a scan rate of 50 mV/s. **c)** BM3h-CNT with 60 mM or 100 mM 2-ketoglutaric acid in a 3 M  $\text{NH}_3/\text{NH}_4^+$  buffer (pH 10) with a scan rate of 200 mV/s. **d)** BM3h-CNT with 100 mM 2-ketoglutaric acid in a 3 M  $\text{NH}_3/\text{NH}_4^+$  buffer (pH 10) with various scan rates. To convert to V vs. RHE, use the equation:  $E_{\text{RHE}} (\text{V}) = E_{\text{Ag/AgCl}} (\text{V}) + 0.210 \text{ V} + 0.059 \text{ V} \times \text{pH} - iR$ .



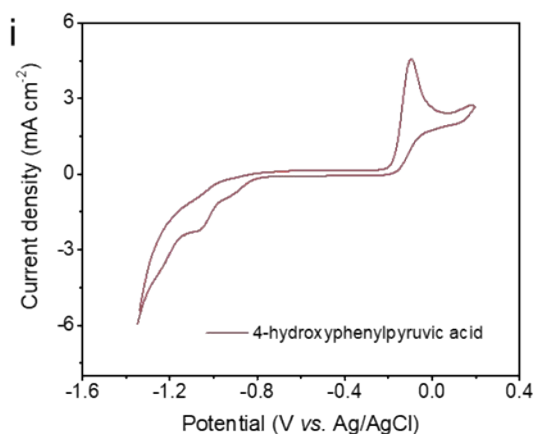


**Figure S16** CV curves of BM3h-CNT with **a)** 60 mM glyoxylic acid, **b)** 60 mM pyruvic acid, **c)** 60 mM 2-ketobutyric acid, **d)** 60 mM oxaloacetic acid, **e)** 60 mM 2-ketoglutaric acid, **f)** 60 mM 2-oxovaleric acid, **g)** 20 mM phenylglyoxylic acid, **h)** 20 mM sodium phenylpyruvate and **i)** 20 mM 4-hydroxyphenylpyruvic acid in a 3 M  $\text{NH}_3/\text{NH}_4^+$  buffer (pH 10) with a scan rate of 10 mV/s. To convert to V vs. RHE, use the equation:  $E_{\text{RHE}} (\text{V}) = E_{\text{Ag/AgCl}} (\text{V}) + 0.210 \text{ V} + 0.059 \text{ V} \times \text{pH} - iR$ .

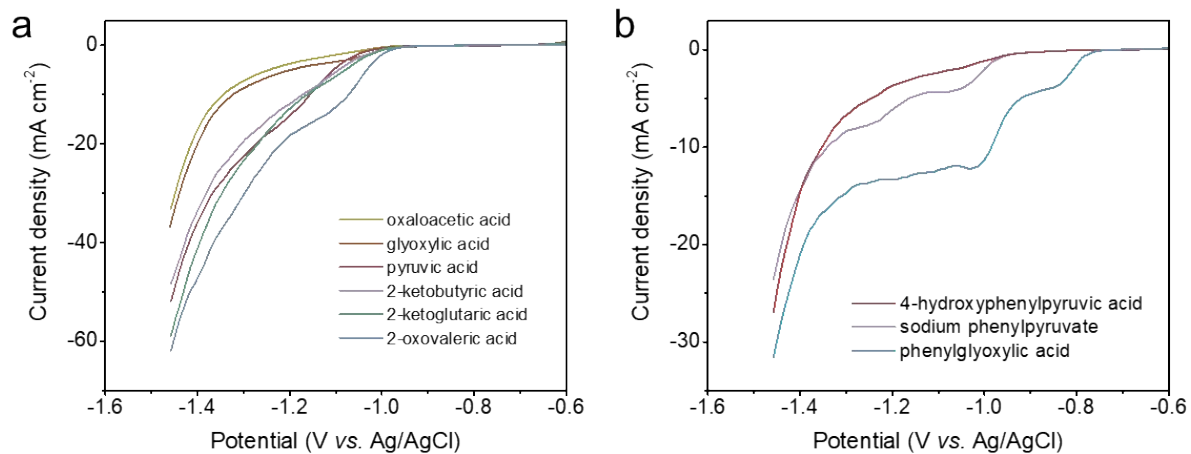


**Figure S17** LSV curves of BM3h-CNT with various substrates in a 3 M  $\text{NH}_3/\text{NH}_4^+$  buffer (pH 10) with a scan rate of 20 mV/s. **a)** 60 mM substrates, **b)** 20 mM substrates. To convert to V vs. RHE, use the equation:  $E_{\text{RHE}} \text{ (V)} = E_{\text{Ag/AgCl}} \text{ (V)} + 0.210 \text{ V} + 0.059 \text{ V} \times \text{pH} - iR$ .

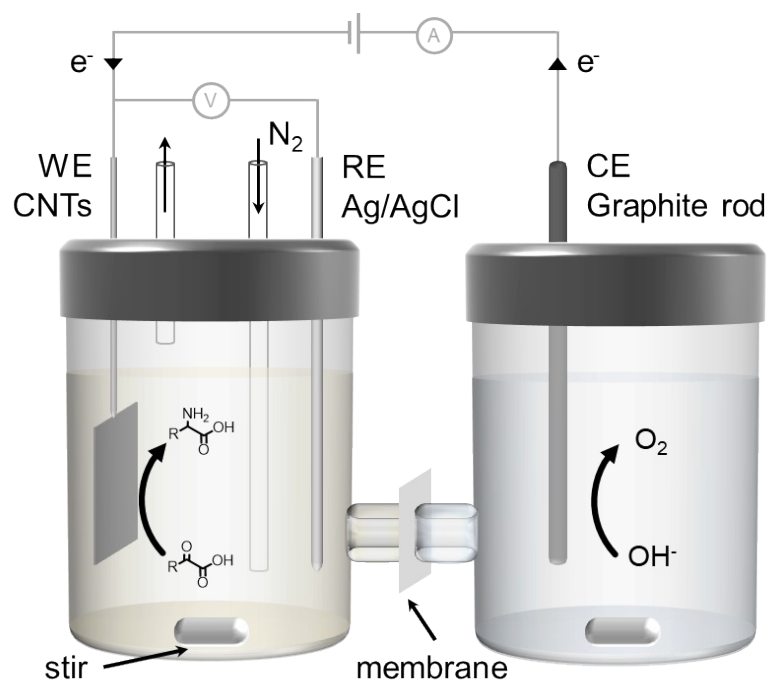
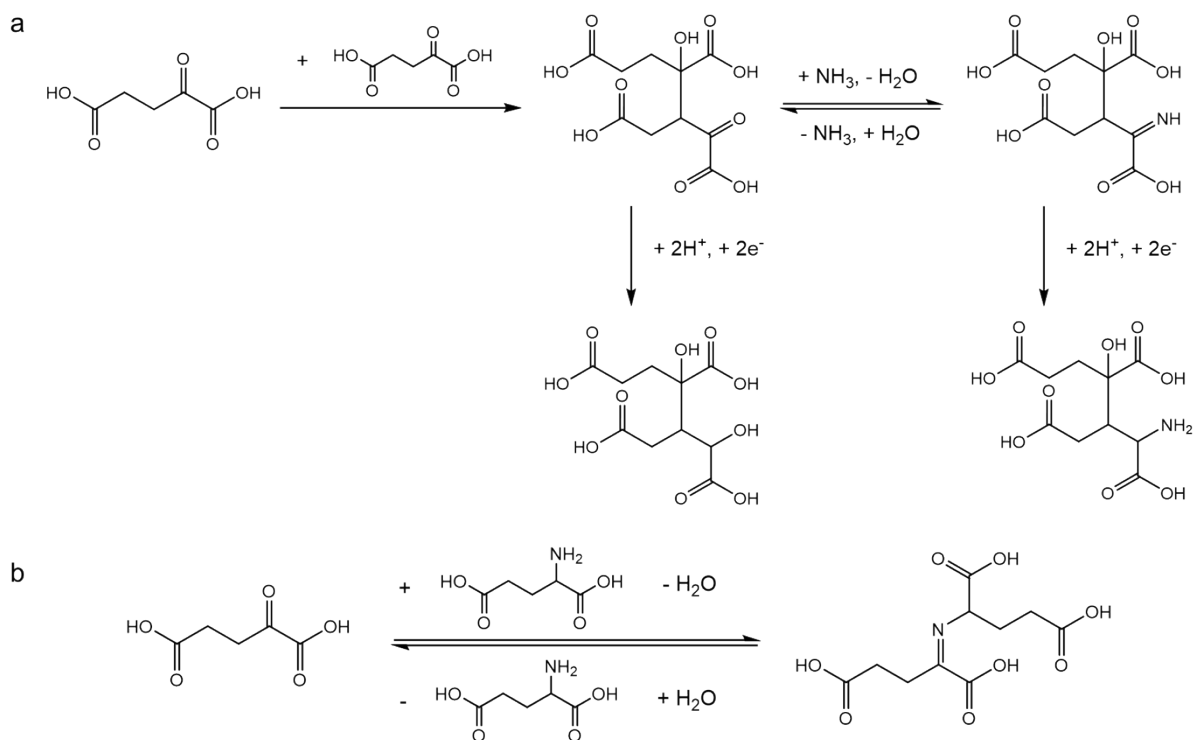
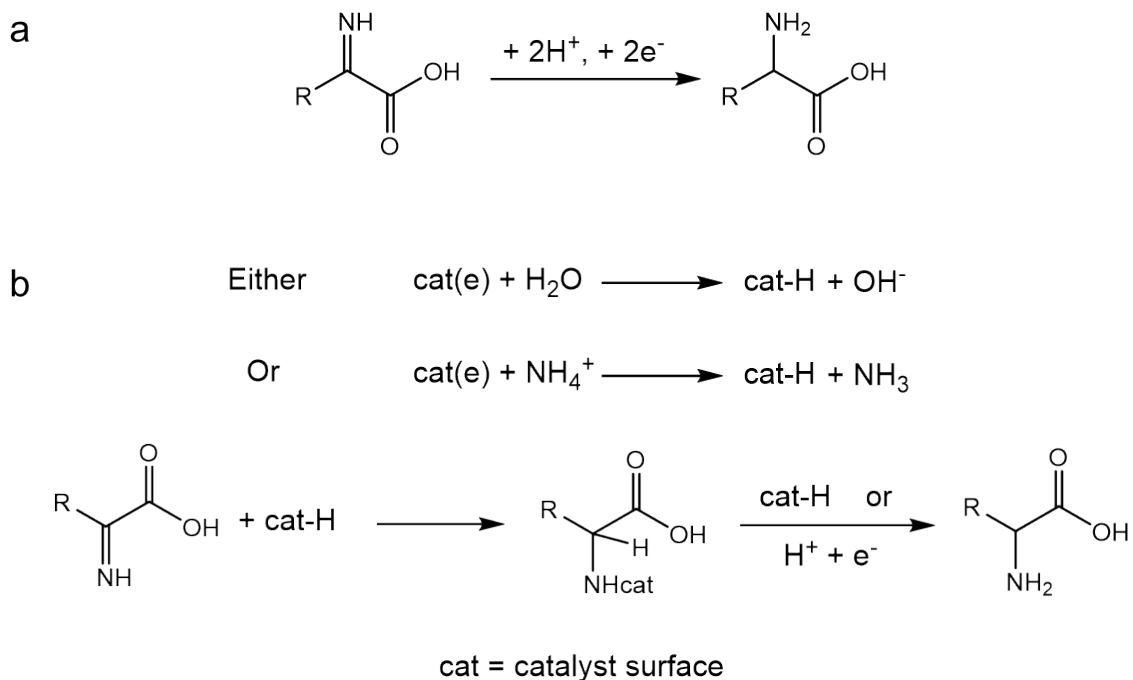


**Figure S18** Schematic diagram of the electrochemical system for amino acids synthesis.



**Scheme S1** Possible reasons for the drop in FE when the concentrations of the substrate were high. **a)** Reduction or reductive amination of the dimer formed by the concurrent condensation of the substrate. **b)** Condensation of the substrate and the product.



**Scheme S2** Two reported possible mechanisms for ERA. **a)** The *in situ* formed imino acid is directly reduced. **b)** The catalyst surface is covered by hydride, then the addition of hydrogen atom to the imino acid occurs.

**Table S1** Comparison of the electrocatalytic amino acids synthesis from keto acids in this work with literature.

Substrate	Catalyst	Nitrogen source	Potential (V vs. RHE)	Duration (h)	Product & FE (%) & Yield (%)	Ref.
2-ketoglutaric acid (100 mM)	BM3h-CNT	NH <sub>3</sub> (6 M)	-0.39	8	glutamic acid	82.6 58.4
2-ketoglutaric acid (60 mM)					glutamic acid	90.0 23.2
2-oxovaleric acid (60 mM)					norvaline	91.3 31.4
oxaloacetic acid (60 mM)					aspartic acid	46.9 2.8
2-ketobutyric acid (60 mM)					2-aminobutyric acid	59.2 11.9
pyruvic acid (60 mM)					alanine	45.0 7.4
glyoxylic acid (60 mM)					glycine	87.4 3.0
phenylglyoxylic acid (20 mM)					phenylglycine	31.4 25.8
phenylpyruvic acid (20 mM)					phenylalanine	92.8 25.9
4-hydroxyphenyl-pyruvic acid (20 mM)					tyrosine	72.9 13.2
oxalic acid (160 mM)	cal. Ti foil	NH <sub>2</sub> OH (192 mM)	-0.7	2	glycine	56 - 1
pyruvic acid (160 mM)	TiO <sub>2</sub> /Ti mesh	NH <sub>3</sub> (6 M)	-0.32	2	alanine	28.7 -
pyruvic acid (160 mM)		NH <sub>2</sub> OH (192 mM)	-0.5		alanine	99 -
glyoxylic acid (160 mM)					glycine	96 -
oxaloacetic acid (160 mM)					aspartic acid	96 -

2-ketoglutaric acid (160 mM)					glutamic acid	95	-	
4-methyl-2-oxovaleric acid (80 mM)					leucine	91	-	
phenylpyruvic acid (20 mM)					phenylalanine	87	-	
4-hydroxyphenylpyruvic acid (20 mM)			-0.6	5	tyrosine	75	-	
2-ketoglutaric acid (10 mM)	Hg	NH <sub>3</sub> (1.24 M)	-0.32	4.5	glutamic acid	-	53	3
phenylglyoxylic acid (70 mM)		NH <sub>3</sub> (5 M)	-0.22	24	2-phenylglycine	91	88	
2-ketoglutaric acid (86 mM)				24	glutamic acid	63	42	
pyruvic acid (93 mM)	Hg		-0.49	18.5	alanine	58	33	4
2-ketobutyric acid (80 mM)		NH <sub>3</sub> (2 M)		25	2-aminobutyric acid	96	48	
2-keto-5-phenylvaleric acid (52 mM)			-0.63	73	2-amino-5-phenylvaleric acid	37	24	
phenylglyoxylic acid (74 mM)	Pd black	NH <sub>3</sub> (15.5 M)	-0.049	24	2-phenylglycine	93	83	
2-ketoglutaric acid (86 mM)	Pt-AA1 *		-0.069	24	glutamic acid	83	64	
pyruvic acid (93 mM)		NH <sub>3</sub> (4.7 M)	-0.029	18.5	alanine	64	37	5
2-ketobutyric acid (80 mM)	Pt-AA2 *	NH <sub>3</sub> (15.5 M)	-0.049	25	2-aminobutyric acid	73	59	
2-keto-5-phenylvaleric acid (52 mM)			-0.069	73	2-amino-5-phenylvaleric acid	56	40	

\* The AA1 electrode consisted of a mixture of Teflon powder and platinum black compressed onto tantalum gauze and the AA2 electrode was similar but was compressed on tantalum expanded metal.

**Table S2** BET surface area of various CNT materials.

Material	BET surface area (m <sup>2</sup> g <sup>-1</sup> )
bulk CNT	189.260
BM1h-CNT	205.583
BM2h-CNT	201.797
BM3h-CNT	197.080
BM4h-CNT	213.756
BM5h-CNT	203.670
N-CNT	47.5474
CNT-NH <sub>2</sub>	202.129

**Table S3** Specifications of the CNT materials.

Material	Outer diameter (nm)	Length ( $\mu\text{m}$ )	Electrical conductivity (S/cm)	Purity (wt.%)	Ash (wt.%)
bulk CNT *	5-18	10-20	-	-	-
N-CNT	30-80	10-30	-	> 95	< 1.5
CNT-NH <sub>2</sub>	8-15	~50	> 100	> 95	-

\* The information for this material is based on our TEM and SEM images due to the lack of details provided by the manufacturer.

## References

1. T. Fukushima and M. Yamauchi, *J. Electroanal. Chem.*, 2021, **51**, 99-106.
2. T. Fukushima and M. Yamauchi, *ChemComm*, 2019, **55**, 14721-14724.
3. A. Anne, S. Danions and J. Moiroux, *New J. Chem*, 1994, **18**, 1169-1174.
4. E. Jeffery and A. Meisters, *Aust. J. Chem.*, 1978, **31**, 73-78.
5. E. Jeffery, O. Johansen and A. Meisters, *Aust. J. Chem.*, 1978, **31**, 79-84.